In Situ Spectroscopic Determination of Faradaic Efficiencies in Systems with Forced Convection under Steady State: Electroreduction of Bisulfite to Dithionite on Gold in an Aqueous...

ARTICLE *in* ANALYTICAL CHEMISTRY · FEBRUARY 1998

Impact Factor: 5.64 · DOI: 10.1021/ac970697f

5 AUTHORS, INCLUDING:

Yuriy Tolmachev
Ftorion
69 PUBLICATIONS **1,014** CITATIONS

SEE PROFILE

Anal. Chem. **1998,** *70,* 1149−1155

In Situ Spectroscopic Determination of Faradaic Efficiencies in Systems with Forced Convection under Steady State: Electroreduction of Bisulfite to Dithionite on Gold in an Aqueous Electrolyte

Yuriy V. Tolmachev, Zhenghao Wang, Yining Hu, In Tae Bae, and Daniel A. Scherson*

Ernest B. Yeager Center for Electrochemical Sciences and the Department of Chemistry, Case Western Reserve University, Cleveland, Ohio 44106-7078

The reduction of bisulfite on Au electrodes in buffered aqueous solutions (pH = 5.25) was examined by in situ near-normal-incidence UV−visible reflection absorption spectroscopy on a rotating disk electrode (RDE) and in situ transmission UV−visible spectroscopy downstream from a channel-type electrode. The currents associated with dithionite ($S_2O_4^{2-}$) formation obtained from the spectroscopic measurements were found to be lower than those expected for a one-electron, diffusion-controlled process. Faradaic efficiencies for $S_2O_4^{2-}$ generation derived from RDE data yielded, in the range −0.60 to −0.75 V vs Ag/AgCl, values close to 100%. The advantages of rotating disk over channel-type electrodes for determining faradaic efficiencies by UV−visible spectroscopic techniques are discussed.

Electrosynthesis provides an expedient route for the industrial production of a variety of high-valued chemicals, including chlorine,[1] adiponitrile,[2] hydroxylamine nitrate,[3] and certain perfluorinated alkanes.[4] In addition to cell design considerations and electrode stability, the *overall* efficiency of these processes is often controlled by the kinetics of heterogeneous electron transfer, as well as by the rates of preceding and subsequent chemical reactions. Of common occurrence are situations in which materials other than the desired product are generated during operation, thereby decreasing the *specific* faradaic efficiencies, i.e., the fraction of the total current (or charge) involved in the generation of a given product.

Quantitative aspects of this phenomenon may be assessed by determining product distributions using conventional analytical techniques external to the reactor or cell. A far more desirable strategy is to acquire such information in situ or on line, i.e., by directly probing the solution adjacent to the electrode surface under well-defined conditions of mass transfer, especially when dealing with rather unstable products. Perhaps the most popular of these methods is the rotating ring−disk electrode (RRDE), in which the ring is used to oxidize or reduce products formed at the disk. The usefulness of this and a few other related electrochemically based techniques may be seriously compromised, however, if the products are not electrochemically active or if the reactions at the ring proceed under partial kinetic control.

Interest in this research group has been focused on the development of in situ and on line spectroscopic techniques capable of providing quantitative information regarding both the identity of electrogenerated products and the potential dependence of their *specific* faradaic yields under well-defined hydrodynamic conditions.[5−9] Closely related spectroelectrochemical techniques for monitoring solution-phase species in the UV−visible range have also been reported in other laboratories both under stagnant[10,11] and, more recently, forced convection conditions using a channel-type cell.[12]

This work illustrates the use of UV−visible spectroscopy at both a rotating disk electrode (RDE), in a reflection absorption geometry, and downstream from a channel-type electrode, in the transmission mode, to determine *specific* faradaic yields of dithionite ($S_2O_4^{2-}$) generation from bisulfite on Au electrodes as a function of the applied potential. All experiments were carried out at pH = 5.25 to mimic conditions found in the large-scale electrosynthesis of $S_2O_4^{2-}$, a widely used bleaching agent in the paper industry.[13] The success of this novel strategy relies in part on the high molar absorptivity of $S_2O_4^{2-}$ in a spectral region readily accessible with conventional instrumentation without interference

(1) Hine, F.; Tilak, B. V.; Viswanathan, K. In *Modern Aspects of Electrochemistry*; White, R. E., Bockris, J. O'M., Conway, B. E., Eds.; Plenum Press: New York, 1986; Vol. 18, p 249.
(2) Danley, D. E. Industrial Electroorganic Chemistry. In *Organic Electrochemistry*, 2nd ed.; Lund, H., Baizer, M. M., Eds.; M. Dekker: New York, 1983; Chapter 30.
(3) Dotson, R. L. *Interface* **1994**, *3*, 35.
(4) Childs, W. V.; Christensen, L.; Klink, F. W.; Kolpin, C. F. Anodic Fluorination in Organic Electrochemistry. In *Organic Electrochemistry: An Introduction and a Guide*, 3rd ed.; Lund, H., Baizer, M. M., Eds.; M. Dekker: New York, 1991; Chapter 26.
(5) Zhao, M.; Scherson, D. A. *Anal. Chem.* **1992**, *64*, 3064.
(6) Wang, Z.; Zhao, M.; Scherson, D. A. *Anal. Chem.* **1994**, *66*, 1993.
(7) Wang, Z.; Zhao, M.; Scherson, D. A. *Anal. Chem.* **1994**, *66*, 4560.
(8) Wang, Z.; Scherson, D. A. *J. Electrochem. Soc.* **1995**, *142*, 4225.
(9) Barbour, R.; Wang, Z.; Bae, I. T.; Tolmachev, Y. V.; Scherson, D. A. *Anal. Chem.* **1995**, *67*, 4024.
(10) (a) Pyun, C.-H.; Park, S. M. *Anal. Chem.* **1986**, *58*, 251. (b) Kim, B. S.; Park, S. M. *J. Electrochem. Soc.* **1995**, *142*, 26; **1995**, *142*, 34.
(11) Jones, D. H.; Hinman, A. S. *Can. J. Chem.* **1996**, *74*, 1403.
(12) (a) Tam, K. Y.; Wang, R. L., Lee, C. W.; Compton, R. G. *Electroanalysis* **1997**, *9*, 219. (b) Wang, R. L.; Tam, K. Y.; Marken, F.; Compton, R. G. *Electroanalysis* **1997**, *9*, 284.
(13) Oloman, C. *J. Electrochem. Soc.* **1970**, *117*, 1604. Gizetdinova, N. A. *J. Appl. Chem. USSR* **1979**, *52*, 2594.

S0003-2700(97)00697-5 CCC: $15.00
Published on Web 02/11/1998

from other species in the media.

The analysis of the data has been based on an approximate, albeit general formalism reported recently in this laboratory,[14] for the evaluation of integrated profiles of stable products in RDE, RRDE, and channel- and tube-type configurations. As shown therein, such an approach serves as a starting point for the theoretical treatment of a variety of on line spectroscopic measurements in well-defined hydrodynamic systems.

THEORY

Near-Normal-Incidence UV−Visible Reflection−Absorption Spectroscopy at a Rotating Disk Electrode. The model herein considered neglects radial components of the flow velocity, as well as contributions to mass transport derived from migration in an electric field, and assumes that the product does not adsorb on the electrode. Under these conditions, the flux of a product P at the surface of a RDE may be expressed in terms of the partial current density due to the formation of P, j_P, as follows:

$$D_P(\mathrm{d}c_P/\mathrm{d}z)_0 = -j_P/(n_P F) \quad (1)$$

In this equation, D_P and c_P are the diffusion coefficient and bulk concentration of P, respectively, z is the coordinate normal to the electrode surface, F is the Faraday constant, and n_P the number of electrons required to form one molecule of P, a parameter defined as negative or positive depending on whether the process is a reduction or an oxidation, respectively. As is customary, the sign of the current is positive for an oxidation and negative for a reduction.

In terms of the dimensionless variable $\zeta_P = z/\delta_P$, where $\delta_P = 1.805\, D_P^{1/3}\nu^{1/6}\omega^{-1/2}$ is the thickness of the diffusion boundary layer for P[15] and other symbols have their common meaning (see List of Symbols). Equation 1 can be rewritten as

$$(\mathrm{d}c_P/\mathrm{d}\zeta_P)_0 = -j_P\delta_P/(n_P F D_P) \quad (2)$$

According to Levich,[15] the solution for the profile of a stable product P, i.e., displaying no decomposition, along an axis normal to the electrode surface at steady state may be expressed in terms of the flux at the surface, i.e.

$$c_P(\zeta_P) = -(\mathrm{d}c_P/\mathrm{d}\zeta_P)_0\int_{\zeta_P}^{\infty}\exp(-u^3)\,\mathrm{d}u = -j_P\delta_P/(n_P F D_P)\int_{\zeta_P}^{\infty}\exp(-u^3)\,\mathrm{d}u \quad (3)$$

For normal-incidence reflection absorption experiments at a RDE, and assuming that the product P is the only optically absorbing species in the media, the absorbance, A, is given by[5]

$$A = 2\epsilon_P\int_0^{\infty}c_P(z)\,\mathrm{d}z = 2\epsilon_P\delta_P\int_0^{\infty}c_P(\zeta_P)\,\mathrm{d}\zeta_P = 2\epsilon_P(\delta_P{}^2/D_P)(j_P/n_P F)\int_0^{\infty}\int_{\zeta_P}^{\infty}\exp(-u^3)\,\mathrm{d}u\,\mathrm{d}\zeta_P \quad (4)$$

where ϵ_P is the molar absorptivity of P. The value of the double integral in the right-hand side of this equation is $\Gamma(2/3)/3$, where $\Gamma(2/3)$ is the gamma function of argument 2/3, which, upon rearrangement, may be shown to yield

$$A\omega/j_P = 2.9408(\epsilon_P/n_P F)(\nu/D_P)^{1/3} \quad (5)$$

Since the right-hand side of eq 5 involves parameters intrinsic either to the product, i.e., ϵ_P, n_P, D_P, or to the solution, ν, the quantity $A\omega/j_P$, is, therefore, constant. In fact, the constancy of this ratio for different potentials, rotation rates, and reactant concentrations may be regarded as proof that the process indeed satisfies the requirements of the model. Note that, in the derivation of eq 5, no restrictions were imposed on the nature of the step limiting the values of j_P, e.g., diffusion, heterogeneous or homogeneous reactions, or a combination of these; hence, this equation is of more general validity than the formulas derived in ref 14.

Transmission Downstream from a Channel-Type Electrode. Concentration profiles of species normal to the electrode surface downstream from the electrode edge of a channel-type cell can be obtained, in general, by using digital simulation techniques of the type implemented Compton and co-workers.[16] It becomes then at least in principle possible to compare experimental absorbance values acquired in transmission along an axis normal to the electrode with working curves obtained once a plausible mechanism has been identified and extract from such an analysis of the kinetic parameters of interest. However, this procedure may not be straightforward even when the actual mechanism is known.

Consider, for example, a simple electrochemical process in which a stable, optically absorbing product P is generated via a heterogeneous irreversible reaction first order in the reactant, R. The reactant may also be consumed via other first-order reactions yielding different products. Within the framework of approximations specified elsewhere,[14] the partial current density for this process averaged over the area of the electrode, denoted as j_P, may be shown to be given by

$$j_P = n_P F D_P\int_0^1 \partial c_P/\partial y(X,0)\,\mathrm{d}X = n_P F D_P[\delta_P(L)\lambda]^{-1}c_R{}^{\infty}\int_0^1\partial\theta/\partial Y(X,0)\,\mathrm{d}X = n_P F D_P\delta_P(L)^{-1}c_R{}^{\infty}\lambda^{-1}J(\sigma) \quad (6)$$

where $X = x/L$, $Y = (2v_o h^2/D_P L)^{1/3}(y/h) = y/\delta_P(L)$, $\theta = \lambda c_P/c_R{}^{\infty}$, L is the electrode length, h is the half-height of the channel, v_o is the linear fluid velocity in the center of the channel, $\delta_P(L) = (D_P L h/2v_o)^{1/3}$, the thickness of the diffusion layer at the down-

(14) Tolmachev, Y. V.; Wang, Z.; Scherson, D. A. *J. Electrochem. Soc.* **1996**, *143*, 3539.

(15) Levich, B. G. *Physicochemical Hydrodynamics*; Prentice Hall: Englewood Cliffs, NJ, 1962.

(16) See, for example: (a) Alden, J. A.; Compton, R. G. *J. Electroanal. Chem.* **1996**, *415*, 1; **1996**, *402*, 1. (b) Compton, R. G.; Pilkington, M. B. G.; Stearn, G. M. *J. Chem. Soc., Faraday Trans. 1* **1988**, *4*, 2155. (c) Fisher, A. C.; Compton, R. G. *J. Phys. Chem.* **1991**, *95*, 7538.

stream edge of the channel electrode L, $\lambda = (k/k_P)(D_P/D_R)^{2/3}$, k the rate constant for the consumption of the reactant, k_P is the rate constant for the formation of the product P, D_R is the diffusion coefficient of R, and $\sigma = (1/3)(\Gamma(1/3)/\Gamma(2/3))^3(Lh/2v_o)(k^3/D_R^2)$ is a dimensionless rate constant. Explicit expressions for the dimensionless flux, $\partial\theta/\partial Y$ and the integrated flux $J(\sigma)$ have been given in eqs 11 and 17 in ref 13.

The absorbance due to P at a dimensionless distance X from the upstream edge of the electrode, assuming, for simplicity, that no other species in the medium absorbs, can be written as follows:

$$A = \epsilon_P \lambda^{-1} \delta_P(L) c_R^{\infty} I(X;\sigma) \quad (7)$$

where $I(X;\sigma)$ is a dimensionless function also defined in ref 13. Therefore, from eqs 6 and 7, the ratio of the absorbance to the partial current becomes

$$A/j_P = (\epsilon_P/n_P F)(hL/2v_o)^{2/3}(D_P)^{-1/3}\{I(X;\sigma)/J(\sigma)\} \quad (8)$$

It becomes evident from this equation that the ratio A/j_P depends on the kinetic parameter σ and, hence, in general, on the applied potential. Although it is possible to determine σ and the faradaic efficiency $\kappa = j_P/j$, where j is the measured current, by finding the best fit of the experimental data, i.e., A/j, to $\kappa I(X;r)/J(\sigma)$ vs X working curves, the results obtained may be subject to large uncertainties, due to lack of sufficient resolution. Furthermore, for more complex mechanisms, such as processes involving proceding chemical reactions, the number of parameters will increase, making determination of κ even less reliable.

EXPERIMENTAL SECTION

Descriptions of the experimental setups, including the optical system and the spectroelectrochemical cells for RDE and channel-type measurements, have been given in refs 5 and 8, respectively. In the case of the RDE, the unpolarized light was incident onto the Au disk of area 0.452 cm^2 of a rotating Au-ring/Au-disk electrode assembly (Pine Instruments, collection efficiency 0.20) using fiber optics at an angle of ~10° with respect to the rotation axis. The error induced by the slight increase in the path length due to such non-normal-incidence conditions may be shown to yield an error no larger than 2%. As specified in ref 8, the gold electrode for the channel-type arrangement was 0.50 cm (length) × 0.60 cm (width), the half-height of the channel 0.16 cm, and the channel width 1.2 cm. For both types of arrangements, the Au working electrode was polished with alumina compounds down to 0.05 μm, the reference electrode was a silver/silver chloride in 3 M NaCl (Bioanalytical Systems), and the counter electrode was a gold foil. All experiments were performed at a temperature of 21 ± 1 °C.

At the beginning of every series of measurements, a 0.50 M solution of NaH_2PO_4 (Fisher, ACS certified in Millipore water) was deaerated in the cell by bubbling nitrogen until the residual oxygen, as judged by the values of the diffusion-limiting currents, reached a concentration of ~1 μM. A precise amount of solid Na_2SO_3 (Fisher, ACS certified) was then introduced into the base electrolyte, keeping the working electrode unpolarized. After dissolution, the solution pH was adjusted to 5.25 with 1 M NaOH. The buffer capacity of this electrolyte was found to be 58 mM/pH unit.

For the spectroelectrochemical experiments, the absorbance A was calculated by using as a reference the light intensity reflected off the RDE surface, or transmitted through the fluid downstream and normal to the plane of the electrode (channel), with the Au working electrode polarized in both cases at a potential positive to the onset of bisulfite reduction (−0.40 V). Measurements at fixed wavelength of 316 nm (monochromator band-pass 2 nm) were performed by scanning the potential at rates in the range of 1−10 mV/s, using the lower values for smaller currents. In order to filter out noise caused by both the instability of the arc lamp and electrode rotation, e.g., surface irregularities, the light intensity was modulated using a chopper at a frequency of ~1.7 kHz.

Potential difference spectra were recorded by stepping the potential from the reference to the sampling values and allowing for the current to achieve steady state (~5 s) before acquisition of optical data.

Determination of the Molar Absorptivity of Dithionite. The actual amount of dithionite in commercial $Na_2S_2O_4$ (Aldrich) was determined by a selective titration technique as described originally by Szekeres.[17] The values obtained, 78.8 ± 0.4%, were slightly lower than that specified by the manufacturer (87.2%). On the basis of cyclic voltammetry and UV−visible spectroscopic measurements, sulfite and thiosulfate were found to be the main impurities. The molar absorptivity of $S_2O_4^{2-}$ was determined by adding a precise amount of solid anhydrous $Na_2S_2O_4$ (20 mg, Aldrich) to 100 mL of a thoroughly degassed solution of 0.2 M KH_2PO_4 and 10 mM Na_2SO_3, pH = 5.25. To avoid exposure to air, a small aliquot of the dithionite solution was delivered with a syringe into a conventional quartz cuvette (1-cm path length) isolated from the atmosphere by a N_2-filled glovebag by puncturing its wall. The cuvette was sealed with adhesive tape prior to opening the bag and rapidly transferred to the spectrophotometer (Varian DMS 200). The same buffered solution without dithionite was used in this case as a reference. Spectra were recorded in the range 370−250 nm, yielding a single prominent feature centered at 316 nm. No changes in the magnitude of the absorbance were observed within 5 min, indicating negligible levels of dithionite decomposition. Based on three independent measurements, the molar absorptivity of dithionite was found to be (7.3 ± 0.3) × 10^6 cm^2/mol, a value that is in agreement with those published elsewhere.[18]

Determination of the Diffusion Coefficient of Dithionite. No limiting currents for dithionite oxidation on Au disk electrodes were found in solutions of 5 mM $Na_2S_2O_4$ in the same buffer as that used in the spectroelectrochemical studies (see below). Similar experiments performed over a range of pH values with solutions of an ionic strength comparable to that employed for bisulfite reduction yielded well-defined limiting currents for $S_2O_4^{2-}$ oxidation in carbonate buffer (0.25 M Na_2CO_3 + 0.25 M $NaHCO_3$, pH = 9.95). The half-wave potential in this case was close to the pH-independent value reported by Cermak and Smutek, i.e., −0.40 V vs SCE.[19]

Based on these measurements, the value of D, assuming a 2-e^- process, was (9.12 ± 0.03) × 10^{-6} cm^2/s, which is similar to those

(17) Szekeres, L. Z. *Anal. Chem.* **1964**, *203*, 1787.
(18) Kosower, E. M.; Bauer, S. W.; *J. Am. Chem. Soc.* **1960**, *82*, 2191. Hagon, E.; Treinin, A.; Wilf, J. *J. Am. Chem. Soc.* **1972**, *94*, 47.
(19) Cermak, V.; Smutek, M. *Collect. Czech. Chem. Commun.* **1975**, *40*, 3241.

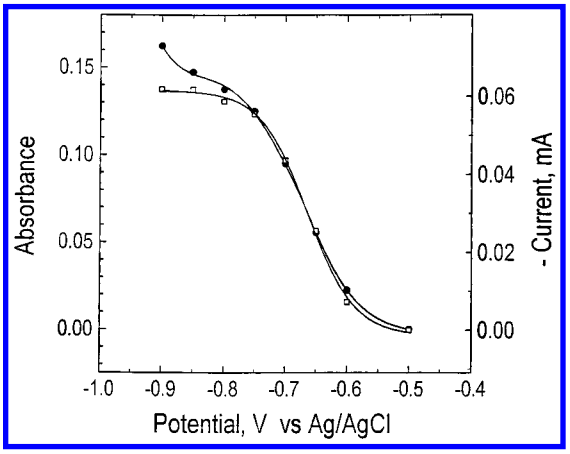

Figure 1. Typical steady-state polarization curve obtained for a gold electrode (length 0.50 cm, width 0.60 cm) in a channel-type cell (half-height 0.16 cm, width, 1.2 cm) in a 10 mM Na_2SO_3 in 0.50 M phosphate buffer solution (pH = 5.25) at a flow rate of 0.32 mL/s, i.e., v_o = 2.5 cm/s (solid circles, right ordinate). The open squares (left ordinate) are the absorbances at 316 nm measured downstream of the electrode as a function of the applied potential. The ordinates were scaled to show the direct proportionality between the current and the amount of dithionite detected spectroscopically in the range −0.50 to −0.75 V (see text for details). The lines represent a polynomial fit to the data.

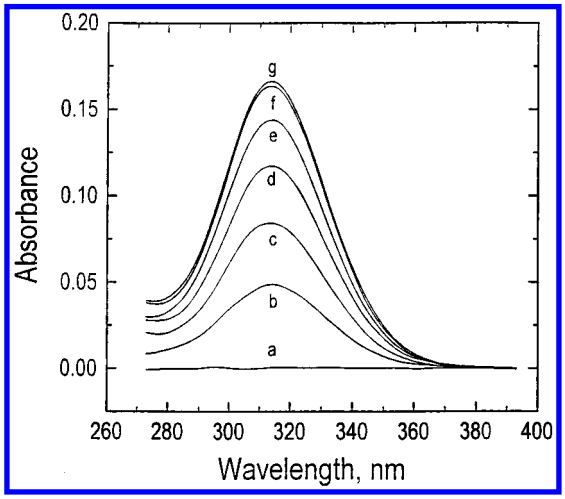

Figure 2. On line potential difference transmission spectra obtained half an electrode length downstream from the electrode edge with the gold electrode polarized at −0.50 (a), −0.65 (b), −0.70 (c), −0.75 (d), −0.8 (e), −0.90 (f), and −1.00 (g) in the same solution under the same conditions described in the caption for Figure 1; reference potential −0.40 V.

reported by other authors,[20] for closely related species, e.g., $S_2O_6^{2-}$, 12.38 × 10^{-6} cm^2/s; $S_2O_8^{2-}$, 11.45 × 10^{-6} cm^2/s; and HSO_3^-, 13.31 × 10^{-6} cm^2/s at infinite dilution. For the case of HSO_3^-, the corresponding value of D in 0.5 M phosphate buffer was determined from the diffusion-limiting current associated with its two-electrode oxidation yielding a value of (6.93 ± 0.02) × 10^{-6} cm^2/s.

RESULTS AND DISCUSSION

Channel-Type Cell. A typical steady-state polarization curve obtained for a gold electrode in a channel-type cell in a 10 mM Na_2SO_3 in 0.5 M phosphate buffer solution (pH = 5.25) at a flow rate of 0.32 mL/s, i.e., v_o = 2.5 cm/s, is shown by the solid circles in Figure 1 (right ordinate). As indicated, this curve exhibits an inflection at ∼ −0.85 V. The current at this potential, ∼65 μA, is far below that expected for a one-electron diffusion-controlled process, i.e., 560 μA.

Unambiguous evidence for generation of dithionite as a product of sulfite reduction on gold was obtained by recording on line the transmission spectrum of the solution half an electrode length downstream from the electrode edge as a function of the applied potential. As shown in Figure 2, a band centered at 316 nm, characteristic of dithionite, could be observed at potentials more negative than −0.50 V, i.e., the onset of the current in Figure 1.

A plot of A at 316 nm as a function of the applied potential is given in open squares in Figure 1 (left ordinate), where the ordinates were scaled to show the direct proportionality that exists between the current and the amount of dithionite detected spectroscopically in the range −0.50 to −0.75 V. Especially noteworthy is the fact that the amount of $S_2O_4^{2-}$ produced reaches a limiting value as indicated by the plateau in Figure 1 (see open squares).

Further experimental data (not shown in this work), revealed linear correlations between the current at the inflection, ∼−0.85 V, and $v_o^{1/3}$, and between the limiting absorbance at λ = 316 nm and $v_o^{-1/3}$ for flow rates in the range 0.05−2 mL/s. However, the slopes of these lines were smaller than those expected for a one-electron diffusion-limited process, and their corresponding intercepts were larger than zero, indicating that the current is not diffusion-controlled.

This overall behavior is in harmony with the results obtained earlier by Kolthoff and Miller[21] and Reynolds and Yuan[22] on a dropping mercury electrode, in which case the better defined waves were also found to be well below diffusion-limited values.

Despite the proportionality between current and absorbance over a rather wide potential range (see Figure 1), no conclusions can be made from these data regarding the faradaic efficiency for $S_2O_4^{2-}$ generation, as the analysis of the data requires prior knowledge of the reaction mechanism. Moreover, even if the heterogeneous electron-transfer process is known to occur via simple first-order kinetics in the reactant, the dependence between the absorbance A and the partial currents j_P for the channel geometry is complex (see eq 8 in Theory), as A/j_P depends on the actual rate. From an overall perspective, on line spectroelectrochemical data of the type shown in Figure 1 acquired under a wide range of conditions, including measurements at various points downstream of the electrode edge, may help elucidate the actual reaction mechanism. However, various models would have to be examined, involving most probably intensive digital simulations, before the most consistent mechanism is identified.

Rotating Disk Electrode. In direct analogy with the behavior found for the channel, polarization curves (j vs E, where j is the total current density) recorded with a Au RDE yielded, at all rotation rates examined, currents at the inflection (see solid lines in panels A−F in Figure 3: (A) 200, (B) 400, (C) 900, (D) 1600, (E) 2500, and (F) 3600 rpm), with values significantly smaller than

(20) Mills, R.; Lobo, V. M. M. *Self-diffusion in Electrolyte Solutions*; Elsevier: Amsterdam, 1989.

(21) Kolthoff, I. M.; Miller, C. S. *J. Am. Chem. Soc.* **1941**, *63*, 2818.
(22) Reynolds, W. L.; Yuan, Y. *Polyhedron* **1986**, *5*, 1467.

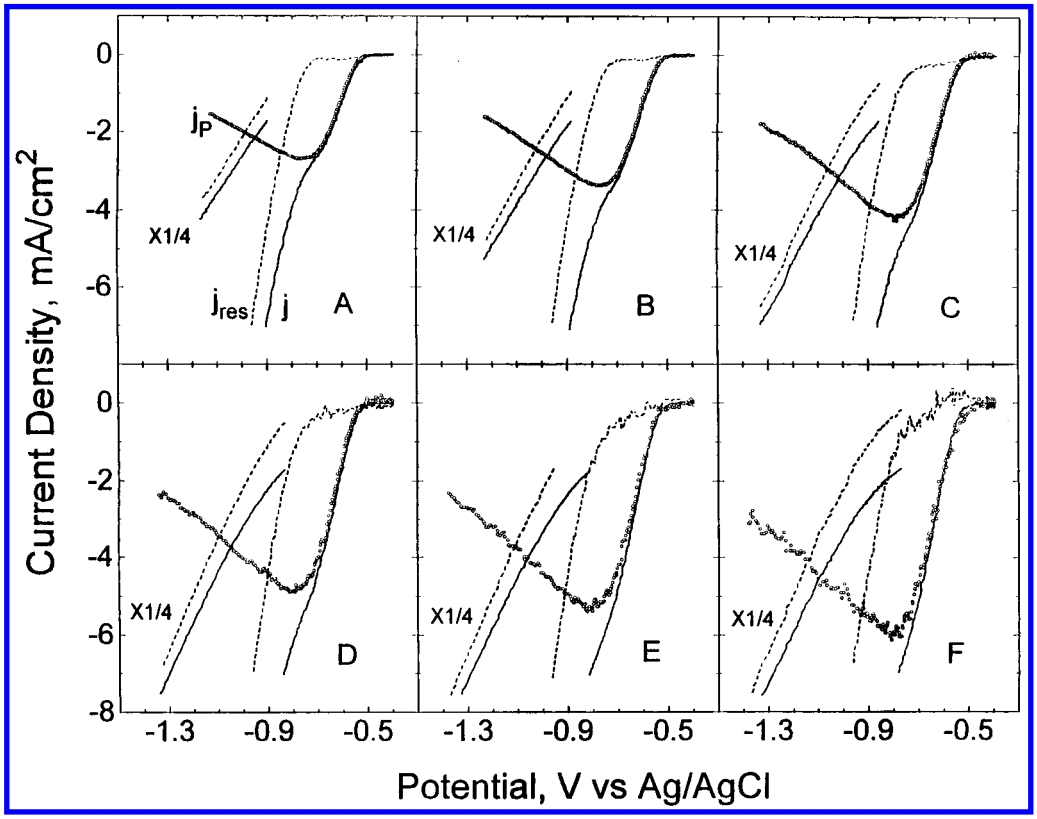

Figure 3. The current density, j (solid line), the partial current density for dithionite generation, j_P (points), and the difference between these two currents, j_{res} (dotted line), obtained with a gold rotating disk (area 0.452 cm^2) of a Au ring−disk electrode in the same solution as that described in the caption to Figure 1 at different rotation rates: (A) 200, (B) 400, (C) 900, (D) 1600, (E) 2500, and (F) 3600 rpm. The values of j_P were calculated from eq 5 based on the absorbance measured in the reflection absorption mode at near-normal incidence at a wavelength of 316 nm (see text for details).

the diffusion-limited currents (j_{lim}) for the two-electron oxidation of sulfite in the same electrolyte at 1.00 V, e.g., $j_{lim} = 19.1$ mA/cm^2 at 900 rpm. Moreover, the position and shape of the dithionite band in the potential difference reflection absorption spectra (not shown) were identical to those obtained in transmission with the channel electrode (see Figure 2), indicating that reflection does not bring about significant spectral artifacts. This may not be surprising, as the reflectance changes induced by the applied potential in the absence of the reactant were smaller than the noise level (5×10^{-4} absorbance units).

Plots of A at $\lambda = 316$ nm vs E recorded during acquisition of the polarization curves in Figure 3 were used to construct j_P vs E plots using eq 5 and are given in scattered form in panels A−F. For these calculations, the constant $A\omega/j_P$ was determined from the values of the molar absorptivity of $S_2O_4^{2-}$, $\epsilon_P = (7.3 \pm 0.3) \times 10^6$ cm^2/mol, and the diffusion coefficient of $S_2O_4^{2-}$, $D_P = (9.12 \pm 0.03) \times 10^{-6}$ cm^2/s, determined in this work, $\nu = 0.010$ cm^2/s, the kinematic viscosity of water, and $n = 2$, yielding a value of 9.9 ± 0.6 rpm·cm^2/mA. Also given in this figure are plots of j_{res} vs E, where j_{res} is the contribution to the total current j due to processes other than bisulfite reduction to dithionite, $j_{res} = j - j_P$.

In the range $-0.60 > E > -0.75$ V, j and j_P were found to virtually coincide, $j_{res} = 0$, providing convincing evidence that j and j_P are not only proportional, as was observed for the channel, but also that the *specific* faradaic efficiency (j_P/j) for dithionite generation under these conditions is within experimental error ~100% (see Figure 4). The decrease in the faradaic efficiency at more positive potentials is caused, most likely, by contributions

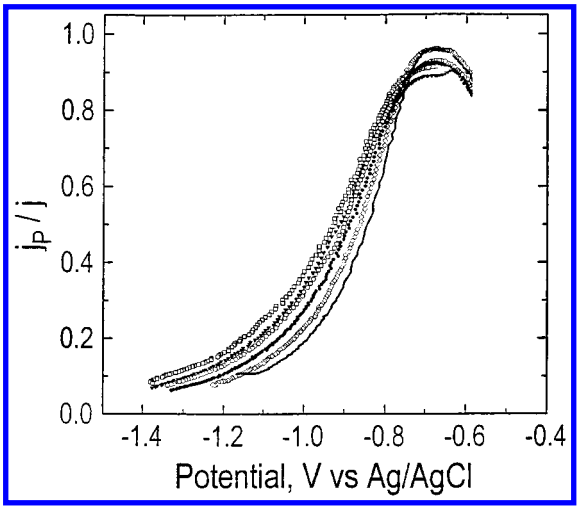

Figure 4. Faradaic efficiency for dithionite generation, i.e., j_P/j, as a function of the applied potential based on the data shown in Figure 3 for six different rotation rates: 200 (solid line), 400 (diamonds), 900 (solid circles), 1600 (open circles), 2500 (solid triangles), and 3600 (open squares) rpm.

to the total current due to the reduction of adventitious oxygen in the solution. Furthermore, j_P increased with ω over the entire potential range, indicating that the reaction proceeds under partial mass transport control. However, despite the increase in j as the potential was made more negative, j_P reached a maximum at ~ -0.80 V (j_P^{max}) at all rotation rates and decreased steadily thereafter.

Plots of j_P^{max} vs $\omega^{1/2}$ and $1/j_P^{max}$ vs $1/\omega^{1/2}$ yielded straight lines with nonzero intercepts, in agreement with the results found for the channel (see above). In addition, j_{res} was found to be independent of ω. This latter behavior is consistent with that expected for hydrogen evolution, a process controlled by heterogeneous electron-transfer kinetics. In fact, the appearance of bubbles on the RDE could be clearly observed in quiescent solutions. The decrease in j_P at $E < -0.85$ V may be caused by a change in the mechanism at more negative potentials to yield species other than dithionite, as suggested by Reynolds and Yuan[22] for mercury electrodes. Alternatively, the higher hydrogen evolution rates would lead to an increase in the local pH, an effect that could reduce the rates of bisulfite reduction, as has been well documented in the literature for pH values in the range 4−6.[21,22]

Also monitored during acquisition of the spectroelectrochemical data was the current at the Au ring, i_{ring}, polarized at a fixed potential in the range −0.30 to +0.10 V. As the disk potential was scanned in the negative direction, i_{ring} yielded a peak in the range −0.85 to −0.95 V of a magnitude 20−30 times smaller than the disk current. This behavior was unlike that observed upon reversing the disk scan direction for which i_{ring} was even smaller.

Large hystereses were also found in experiments in which the ring potential was scanned, while the disk potential was held fixed in the range −0.60 to −1.0 V. The currents at the peak observed during the scan in the positive direction were at least 3 times smaller than the expected diffusion-limited currents based on the value of the collection efficiency. A similar behavior was found in other experiments involving the oxidation of 5 mM $Na_2S_2O_4$ dithionite on a Au disk electrode in the same buffer solution, which again yielded values for the peak current ∼3 times smaller than those predicted for the diffusion-limiting current. It may be concluded on the basis of these purely electrochemical data that the information derived from the RRDE technique for the system under study is of very limited value.

SUMMARY

This work examined the use of UV−visible spectroscopy in the presence of convective flow for the detection of an optically absorbing solution-phase product generated at an electrode surface, using the reduction of bisulfite (HSO_3^-) to dithionite ($S_2O_4^{2-}$) on Au in aqueous buffered solutions (pH = 5.25) as a model system. The rate-determining step for this process appears to be the homogeneous formation of SO_2, the electrochemically reactive species, from HSO_3^-; hence, the observed limiting currents are not controlled purely by mass transport. Under these conditions, it would be very problematic, from both experimental and theoretical viewpoints, to extract the fraction of the total current (which contains sizable contributions derived from hydrogen evolution at more negative potentials) due to dithionite generation by using hydrodynamic modulation at a RDE.[23] Furthermore, attempts to measure faradaic efficiencies for the $HSO_3^-/S_2O_4^{2-}$ using a rotating ring−disk electrode proved unsuccessful, because the ring currents due to dithionite oxidation were found to be below diffusion-limiting values in the entire potential range accessible to these measurements. High sensitivities were observed by employing both near-normal-incidence reflection absorption at a rotating disk electrode and transmission downstream from a channel-type electrode for the identification of $S_2O_4^{2-}$, a species that displays a prominent absorption band centered at 316 nm ($\epsilon \approx 10^7$ cm^2/mol). However, definitive advantages were found for the RDE over the channel-type electrode for the quantitative determination of faradaic efficiencies; i.e., A/j_P for the RDE (see eq 5) is independent of the mechanism and kinetics of the heterogeneous process that generates the optically absorbing product. Quantitative measurements yielded for the $S_2O_2^{2-}$ values of κ close to 100% in the range −0.60 to −0.75 V vs Ag/AgCl.

(23) Miller, B.; Bruckenstein, S. *Anal. Chem.* **1974**, *46*, 2026.

ACKNOWLEDGMENT

This work was supported by the Advanced Research Projects Agency, ONR Contract No. N00014-92-J-1848.

LIST OF SYMBOLS

A	absorbance
c_i	concentration of species i
D_i	diffusion coefficient of species i
F	Faraday constant
h	half-height of the channel electrode cell
$I(X;\sigma)$	dimensionless function proportional to the absorbance downstream from a channel-type cell
$J(\sigma)$	integrated dimensionless flux on the channel electrode
j	current density
j_i	partial current due to the formation of i from R
k	heterogeneous rate constant for reaction that consumes the reactant
k_i	heterogenenous rate constant for formation of species i
n_P	number of electrons required to form one molecule of P from the reactant(s)
L	length of the channel electrode
P	product
R	reactant
v_o	fluid velocity in the center of the channel-type cell
x	coordinate in the direction of the flow in a channel electrode
X	(= x/L) dimensionless distance in the direction of fluid flow for a channel-type cell
y	coordinate normal to the surface of an electrode in a channel-type cell
Y	dimensionless coordinate normal to the surface of an electrode in a channel-type cell
z	coordinate normal to the surface of a RDE
δ_i	(= 1.805 $D_i^{1/3}\nu^{1/6}\omega^{-1/2}$) thickness of the diffusion boundary layer of species i
ϵ_i	molar absorptivity of species i
ζ_i	(= z/δ_i) dimensionless coordinate normal to the surface of RDE
κ	(= j_P/j) faradaic efficiency
λ	(= $(k/k_P)(D_P/D_R)^{2/3}$) dimensionless parameter

ν kinematic viscosity of the solution

σ $(= (1/3)(\Gamma(1/3)/\Gamma(2/3))^3(1h/2v_o)(k^3/D_R^2))$ dimensionless heterogeneous rate constant

θ $(= \lambda c_P/c_R^\infty)$ dimensionless concentration

ω rotation rate of the RDE (rad/s)

Received for review July 2, 1997. Accepted December 15, 1997.

AC970697F